Proceedings of the 1999 IEEE
International Conference on Robotics & Automation
Detroit, Michigan • May 1999

Trajectory Tracking Control of a Four-Wheel Differentially Driven Mobile Robot

Luca Caracciolo Alessandro De Luca Stefano Iannitti

Dipartimento di Informatica e Sistemistica
Università degli Studi di Roma "La Sapienza"
Via Eudossiana 18, 00184 Roma, Italy
{deluca}@labrob.ing.uniroma1.it

Abstract

We consider the trajectory tracking control problem for a 4-wheel differentially driven mobile robot moving on an outdoor terrain. A dynamic model is presented accounting for the effects of wheel skidding. A model-based nonlinear controller is designed, following the dynamic feedback linearization paradigm. An operational nonholonomic constraint is added at this stage, so as to obtain a predictable behavior for the instantaneous center of rotation thus preventing excessive skidding. The controller is then robustified, using conventional linear techniques, against uncertainty in the soil parameters at the ground-wheel contact. Simulation results show the good performance in tracking spline-type trajectories on a virtual terrain with varying characteristics.

1 Introduction

Robotic autonomous navigation tasks in outdoor environments can be effectively performed by skid-steering vehicles [1]. Typically, these are 4-wheel differentially driven (4wdd) vehicles in which rotational motion is achieved by a differential thrust on wheel pairs at opposite sides. One commercial example is the ATRV-2 mobile robot by RWI (see Fig. 1). The absence of a steering system makes 4wdd vehicles mechanically robust and able to move on rough terrains with ease and good maneuverability. In applications where the robot needs to move also on paved grounds, skid-steering vehicles are preferred to tracked vehicles because they do not corrupt the contact surface. Although the dynamic behavior of 4wdd skid-steering vehicles is similar to that of vehicles with tracks, the literature on autonomous navigation has focused mostly on the latter class [2, 3].

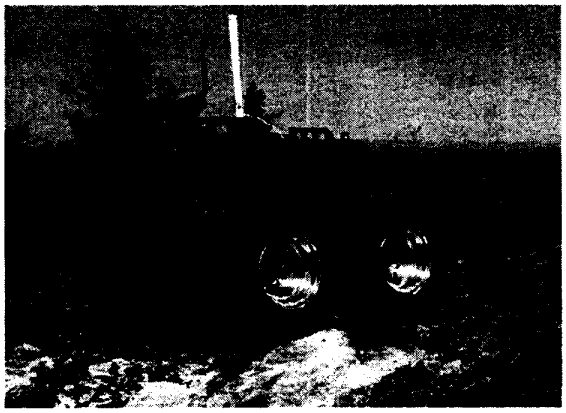

Figure 1: ATRV-2 mobile robot

When considering the problem of accurate trajectory tracking, 4wdd vehicles are quite difficult to control. In fact, in order to follow a curved path, the wheels need to skid laterally and cannot be tangent to the desired path. Moreover, the instantaneous center of rotation (ICR) of 4wdd vehicles may move out of the robot wheelbase, causing loss of motion stability This is different from car-like vehicles, whose ICR is always theoretically fixed along the rear wheels axis [4]. From the modeling point of view, the equilibrium equation of the forces orthogonal to the wheels should be taken into account and this prescribes the use of a dynamic model for control design purposes, instead of a simpler kinematic one.

In this paper, we present a robust trajectory tracking control system for 4wdd vehicles. After deriving a dynamic model of a 4wdd vehicle, we design a model-based tracking controller, by borrowing an approach used for motion planning and control of nonholonomic

0-7803-5180-0-5/99 $10.00 © 1999 IEEE

wheeled mobile robots [4, 5]. The basic idea is to specify the longitudinal coordinate of the ICR, in order to force it to remain inside the robot wheelbase. Adding this operational kinematic constraint, we proceed with full linearization of the system via dynamic state feedback. The obtained closed-loop system is linear and input-output decoupled, thus stabilization to a desired trajectory is easily achieved by means of linear control techniques. However, the overall nonlinear control law depends on soil parameters [3]. We study the effects of uncertain soil parameters on the dynamics of the closed-loop system with respect to a specific class of trajectories and propose then a robust control scheme that reject these disturbances. Simulation results on tracking of robot trajectories over a virtual terrain characterized by varying parameters are finally presented.

2 Dynamic Modeling

We develop a vehicle dynamic model useful for control design, neglecting some side effects introduced, e.g., by suspensions and tire deformation (see, e.g., [6]). In particular, we make the following assumptions:

1. Rigid vehicle moving on a horizontal plane.
2. Vehicle speed below 10 km/h (about 6 mph).
3. Longitudinal wheel slippage neglected.
4. Tire lateral force function of its vertical load.

2.1 Skid-steering motion analysis

Define a fixed reference frame $F(X, Y)$ and a moving frame $f(x, y)$ attached to the vehicle body, with origin at the vehicle center of mass G (see Fig. 2). The center of mass is located at distances a and b (usually, $a < b$) from the front and rear wheels axes, respectively, and is symmetric with respect to the vehicle sides (at distance t).

Let $\dot{x}$, $\dot{y}$, $\dot{\theta}$ be, respectively, the longitudinal, lateral, and angular velocity of the vehicle in frame f. In the fixed frame F, the absolute velocities are

$$\begin{bmatrix} \dot{X} \\ \dot{Y} \end{bmatrix} = \begin{bmatrix} \dot{x}\cos\theta - \dot{y}\sin\theta \\ \dot{x}\sin\theta + \dot{y}\cos\theta \end{bmatrix} = R(\theta) \begin{bmatrix} \dot{x} \\ \dot{y} \end{bmatrix}.$$

Differentiation with respect to time gives

$$\begin{bmatrix} \ddot{X} \\ \ddot{Y} \end{bmatrix} = R(\theta) \begin{bmatrix} \ddot{x} - \dot{y}\dot{\theta} \\ \ddot{y} + \dot{x}\dot{\theta} \end{bmatrix} = R(\theta) \begin{bmatrix} a_x \\ a_y \end{bmatrix},$$

where a_x and a_y are the absolute accelerations expressed in the moving frame f. At each instant the vehicle motion is a pure rotation around a point C, the instantaneous center of rotation, in which the linear velocity components in f vanish. Its coordinates are

$$\begin{bmatrix} x_c \\ y_c \end{bmatrix} = \begin{bmatrix} -\dot{y}/\dot{\theta} \\ \dot{x}/\dot{\theta} \end{bmatrix}.$$

The angular velocity $\dot{\theta}$ and the lateral velocity $\dot{y}$ both vanish during straight line motion, and the ICR goes to infinity along the y-axis. On a curved path, the ICR shifts (forwards) by an amount $|x_c|$. When $\dot{y} = 0$, there is no lateral skidding. If x_c goes out of the robot wheelbase, the vehicle skids dramatically with loss of motion stability.

Finally, note that the longitudinal velocity $\dot{x}_i$ and the lateral (skidding) velocity $\dot{y}_i$ of each wheel ($i = 1, \ldots, 4$) are given by

$$\begin{array}{rcll} \dot{x}_1 = \dot{x}_4 & = & \dot{x} - t\dot{\theta} & \text{(left)} \\ \dot{x}_2 = \dot{x}_3 & = & \dot{x} + t\dot{\theta} & \text{(right)} \\ \dot{y}_1 = \dot{y}_2 & = & \dot{y} + a\dot{\theta} & \text{(front)} \\ \dot{y}_3 = \dot{y}_4 & = & \dot{y} - b\dot{\theta} & \text{(rear).} \end{array} \quad (1)$$

2.2 Equations of motion

The free-body diagram of forces and velocities is shown in Fig. 2, with the vehicle having instantaneous positive velocity components $\dot{x}$ and $\dot{\theta}$ and negative velocity $\dot{y}$. Wheels develop tractive forces F_{xi} and are subject to longitudinal resistance forces R_{xi}, for $i = 1, \ldots, 4$. We assume that wheel actuation is equal on each side so as to reduce longitudinal slip. Thus, it will always be $F_{x4} = F_{x1}$ and $F_{x3} = F_{x2}$. Lateral forces F_{yi} act on the wheels as a consequence of lateral skidding. Also, a resistive moment M_r around the center of mass is induced in general by the F_{yi} and R_{xi} forces.

For a vehicle of mass m and inertia I about its center of mass, the equations of motion can be written in frame f as:

$$\begin{array}{rcl} ma_x & = & 2F_{x1} + 2F_{x2} - R_x \\ ma_y & = & -F_y \\ I\ddot{\theta} & = & 2t(F_{x1} - F_{x2}) - M_r. \end{array} \quad (2)$$

To express the longitudinal resistive force R_x, the lateral resistive force F_y, and the resistive moment M_r, we should consider how the vehicle gravitational load mg is shared among the wheels and introduce a Coulomb friction model for the wheel-ground contact. We have

$$\begin{array}{rcl} F_{z1} = F_{z2} & = & \dfrac{b}{a+b} \cdot \dfrac{mg}{2} \\ F_{z3} = F_{z4} & = & \dfrac{a}{a+b} \cdot \dfrac{mg}{2}. \end{array}$$

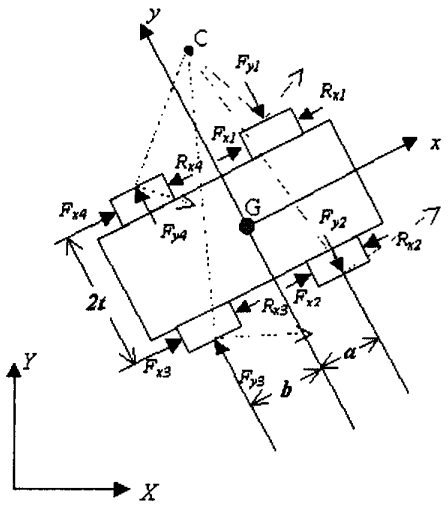

Figure 2: Free-body diagram

At low speed, the lateral load transfer due to centrifugal forces on curved paths can be neglected. In case of hard ground, we can assume that the contact patch between wheel and ground is rectangular and that the tire vertical load produces an uniform pressure distribution. In this condition, $R_{xi} = f_r F_{zi} \mathrm{sgn}(\dot{x}_i)$, where f_r is the coefficient of rolling resistance, assumed independent from velocity [7]. The total longitudinal resistive force is then

$$R_x = \sum_{i=1}^{4} R_{xi} = f_r \frac{mg}{2} \left(\mathrm{sgn}(\dot{x}_1) + \mathrm{sgn}(\dot{x}_2)\right). \quad (3)$$

Introducing a lateral friction coefficient μ, the lateral force acting on each wheel will be $F_{yi} = \mu F_{zi} \mathrm{sgn}(\dot{y}_i)$. The total lateral force is thus

$$F_y = \sum_{i=1}^{4} F_{yi} = \mu \frac{mg}{a+b} \left(b\,\mathrm{sgn}(\dot{y}_1) + a\,\mathrm{sgn}(\dot{y}_3)\right), \quad (4)$$

while the resistive moment is

$$\begin{aligned} M_r &= a(F_{y1} + F_{y2}) - b(F_{y3} + F_{y4}) \\ &\quad + t\left[(R_{x2} + R_{x3}) - (R_{x1} + R_{x4})\right] \\ &= \mu \tfrac{abmg}{a+b} \left(\mathrm{sgn}(\dot{y}_1) - \mathrm{sgn}(\dot{y}_3)\right) \\ &\quad + f_r \tfrac{tmg}{2} \left(\mathrm{sgn}(\dot{x}_2) - \mathrm{sgn}(\dot{x}_1)\right). \end{aligned} \quad (5)$$

The dynamic model can be rewritten in frame F, introducing the generalized coordinates $q = (X, Y, \theta)$ and matrix notation

$$M\ddot{q} + c(q, \dot{q}) = E(q)\tau, \quad (6)$$

with

$$M = \begin{bmatrix} m & 0 & 0 \\ 0 & m & 0 \\ 0 & 0 & I \end{bmatrix}, \quad c(q,\dot{q}) = \begin{bmatrix} R_x \cos\theta - F_y \sin\theta \\ R_x \sin\theta + F_y \cos\theta \\ M_r \end{bmatrix}$$

and

$$E(q) = \begin{bmatrix} \cos\theta/r & \cos\theta/r \\ \sin\theta/r & \sin\theta/r \\ t/r & -t/r \end{bmatrix}, \quad \tau_i = 2rF_{xi} \ (i = 1, 2),$$

being r the wheel radius, τ_1 and τ_2 the torques produced by the left and right side motors at the load side, respectively. An ideal transmission factor is also assumed.

3 Trajectory Control

3.1 Operative nonholonomic constraint

We start by observing that x_c (the x-axis projection of the instantaneous center of rotation) cannot be larger than a. If this happens, the vehicle would skid along the y-axis thus losing control. In order to have the vehicle move properly, one should have then

$$\left| -\frac{\dot{y}}{\dot{\theta}} \right| < a.$$

Therefore, we can introduce the following operative constraint

$$\dot{y} + d_0\dot{\theta} = 0, \quad 0 < d_0 < a,$$

or, in terms of generalized coordinates,

$$\begin{bmatrix} -\sin\theta & \cos\theta & d_0 \end{bmatrix} \begin{bmatrix} \dot{X} \\ \dot{Y} \\ \dot{\theta} \end{bmatrix} = A(q)\dot{q} = 0. \quad (7)$$

This relation represents a nonholonomic constraint that can be attached to the dynamic model (6) for control design purposes. When this constraint is enforced, the robot dynamics becomes

$$M\ddot{q} + c(q, \dot{q}) = E(q)\tau + A^T(q)\lambda, \quad (8)$$

where λ is the vector of Lagrange multipliers corresponding to eq. (7).

Admissible generalized velocities $\dot{q}$ can be expressed as

$$\dot{q} = S(q)\eta, \quad \eta \in I\!R^2, \quad (9)$$

where η is a pseudo-velocity and $S(q)$ is a 3×2 full rank matrix, whose columns are in the null space of $A(q)$, e.g.,

$$S(q) = \begin{bmatrix} \cos\theta & -\sin\theta \\ \sin\theta & \cos\theta \\ 0 & -\frac{1}{d_0} \end{bmatrix}.$$

We can differentiate (9) and eliminate λ from eq. (8) so as to obtain the reduced dynamic model (dropping dependencies)

$$\begin{aligned} \dot{q} &= S\eta \\ \dot{\eta} &= \left(S^T M S\right)^{-1} S^T \left(E\tau - M\dot{S}\eta - c\right). \end{aligned} \tag{10}$$

3.2 Partially linearizing static feedback

Following [8], if we apply the nonlinear static state-feedback law

$$\tau = \left(S^T E\right)^{-1} \left(S^T M S u + S^T M \dot{S}\eta + S^T c\right), \tag{11}$$

where $u = (u_1, u_2)$ is the vector of new control variables, system (10) becomes a purely (second-order) kinematic model

$$\begin{aligned} \dot{q} &= S\eta \\ \dot{\eta} &= u. \end{aligned}$$

In our case, the control law (11) has the explicit form

$$\begin{bmatrix} \tau_1 \\ \tau_2 \end{bmatrix} = \begin{bmatrix} \frac{r}{2}\left(mu_1 + \frac{m}{d_0}\eta_2^2 + R_x\right) \\ -\frac{rd_0}{2t}\left(\left(m + \frac{I}{d_0^2}\right)u_2 - \frac{m}{d_0}\eta_1\eta_2 + F_y - \frac{M_r}{d_0}\right) \\ \frac{r}{2}\left(mu_1 + \frac{m}{d_0}\eta_2^2 + R_x\right) \\ +\frac{rd_0}{2t}\left(\left(m + \frac{I}{d_0^2}\right)u_2 - \frac{m}{d_0}\eta_1\eta_2 + F_y - \frac{M_r}{d_0}\right) \end{bmatrix} \tag{12}$$

and gives

$$\begin{aligned} \dot{X} &= \cos\theta\,\eta_1 - \sin\theta\,\eta_2 \\ \dot{Y} &= \sin\theta\,\eta_1 + \cos\theta\,\eta_2 \\ \dot{\theta} &= -\tfrac{1}{d_0}\,\eta_2 \\ \dot{\eta}_1 &= u_1 \\ \dot{\eta}_2 &= u_2. \end{aligned} \tag{13}$$

3.3 Fully linearizing dynamic feedback

We show next that, by choosing a particular output, eqs. (13) can be fully linearized and input-output decoupled by means of a dynamic state feedback.

For, we choose as linearizing outputs the position of a point D placed on the x-axis at a distance d_0 from the vehicle frame origin

$$z = \begin{bmatrix} X + d_0\cos\theta \\ Y + d_0\sin\theta \end{bmatrix}, \tag{14}$$

and add one integrator on the input u_1 (dynamic extension)

$$\begin{aligned} u_1 &= \xi \\ \dot{\xi} &= v_1 \\ u_2 &= v_2, \end{aligned} \tag{15}$$

where ξ is the controller state and v_1 and v_2 are the new control inputs.

By applying the standard input-output decoupling algorithm (see, e.g., [9]), we differentiate eq. (14) until the input v explicitly appears. We obtain

$$\begin{aligned} \ddot{z} &= \begin{bmatrix} \cos\theta & \frac{1}{d_0}\eta_1\sin\theta \\ \sin\theta & -\frac{1}{d_0}\eta_1\cos\theta \end{bmatrix} v \\ &\quad + \begin{bmatrix} \frac{2}{d_0}\xi\eta_2\sin\theta - \frac{1}{d_0^2}\eta_1\eta_2^2\cos\theta \\ -\frac{2}{d_0}\xi\eta_2\cos\theta - \frac{1}{d_0^2}\eta_1\eta_2^2\sin\theta \end{bmatrix} \\ &= \alpha(q,\eta)v + \beta(q,\eta). \end{aligned}$$

Since

$$\det\left[\alpha(q,\eta)\right] = -\frac{1}{d_0}\,\eta_1,$$

we have that the decoupling matrix α is nonsingular iff the vehicle longitudinal velocity η_1 is different from zero. Whenever defined, the control law

$$v = \alpha^{-1}(q,\eta)\left[r - \beta(q,\eta)\right], \tag{16}$$

where r is the trajectory jerk reference, yields

$$\dddot{z} = r, \tag{17}$$

i.e., two independent input-output chains of three integrators.

Combining eqs. (15) and (16) gives the following input-output decoupling and fully linearizing dynamic controller

$$\begin{aligned} \dot{\xi} &= \cos\theta\, r_1 + \sin\theta\, r_2 + \tfrac{1}{d_0^2}\eta_1\eta_2^2 \\ u_1 &= \xi \\ u_2 &= \tfrac{d_0}{\eta_1}\left(\sin\theta\, r_1 - \cos\theta\, r_2\right) - \tfrac{2}{\eta_1}\xi\eta_2. \end{aligned} \tag{18}$$

We note that the limitation $\eta_1 \neq 0$ does not avoid to achieve good tracking performance by means of controller (18), as long as the trajectory is persistent.

3.4 Linear stabilization for tracking

It is easy to complete the control design for eq. (17) using a exponentially stabilizing state feedback for each integrator chain with input r_i. For $i = 1, 2$, we choose

$$r_i = \dddot{z}_{di} + k_{ai}(\ddot{z}_{di} - \ddot{z}_i) + k_{vi}(\dot{z}_{di} - \dot{z}_i) + k_{pi}(z_{di} - z_i), \tag{19}$$

where the gains are such that $\lambda^3 + k_{ai}\lambda^2 + k_{vi}\lambda + k_{pi}$ $(i = 1, 2)$ are Hurwitz polynomials, $z_d(t)$ is the desired smooth reference trajectory, and z, $\dot{z}$ and $\ddot{z}$ can be evaluated in terms of q, η and ξ.

The state-feedback control law (19) can be seen as an output-feedback linear controller having two (realizable) minimum-phase zeros, characterized by the

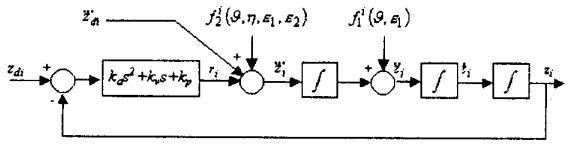

Figure 3: Linear control scheme for tracking

gain ratios k_v/k_a and k_p/k_a, and a feedforward action depending on $\ddot{z}_d$ (see Fig. 3). The resulting control scheme has the open-loop transfer function

$$F(s) = C(s) \cdot P(s) = (k_a s^2 + k_v s + k_p) \cdot \frac{1}{s^3}. \quad (20)$$

4 Robust Control Design

In case of perfect knowledge of the ground-wheel contact parameters, the control law (12) perfectly compensates for the terrain factors and leads to the kinematic system (13) for which trajectory tracking is easily achieved by means of the dynamic controller (18) and the stabilizer (19).

When R_x, F_y, and M_r are unknown (because of μ and f_r) or just incorrectly estimated, the vehicle closed-loop dynamics will still be nonlinear and coupled. The influence of an error on the terrain factors estimate is a torque disturbance that should be rejected by a proper robust control design.

4.1 Disturbance analysis

Let $\hat{R}_x$, $\hat{F}_y$, $\hat{M}_r$ be the estimated values of the terrain factors. Then, the implementable control law is still given by (12) with these estimates in place of the real values. The resulting system, in place of (13), is

$$\begin{aligned} \dot{X} &= \cos\theta\,\eta_1 - \sin\theta\,\eta_2 \\ \dot{Y} &= \sin\theta\,\eta_1 + \cos\theta\,\eta_2 \\ \dot{\theta} &= -\tfrac{1}{d_0}\,\eta_2 \\ \dot{\eta}_1 &= u_1 + \epsilon_1 \\ \dot{\eta}_2 &= u_2 + \epsilon_2, \end{aligned} \quad (21)$$

where

$$\begin{aligned} \epsilon_1 &= \frac{1}{m}\left(\hat{R}_x - R_x\right) \\ \epsilon_2 &= \frac{d_0^2}{m d_0^2 + I}\left(\left(\hat{F}_y - \frac{\hat{M}_r}{d_0}\right) - \left(F_y - \frac{M_r}{d_0}\right)\right). \end{aligned}$$

If we suppose that the vehicle moves on a (unknown) uniform terrain, the above disturbances will be constant.

When we apply the dynamic controller (18), ϵ_1 and ϵ_2 will affect the resulting nominal integrator chains (17) in a special way. Beside the output (14), we have

$$\begin{aligned} \dot{z} &= \begin{bmatrix} \cos\theta\,\eta_1 \\ \sin\theta\,\eta_1 \end{bmatrix} \\ \ddot{z} &= \begin{bmatrix} \xi\cos\theta + \frac{1}{d_0}\eta_1\eta_2\sin\theta \\ \xi\sin\theta - \frac{1}{d_0}\eta_1\eta_2\cos\theta \end{bmatrix} + \begin{bmatrix} \cos\theta \\ \sin\theta \end{bmatrix}\epsilon_1, \end{aligned}$$

and

$$\dddot{z} = r + \begin{bmatrix} \frac{2}{d_0}\eta_2\sin\theta & \frac{1}{d_0}\eta_1\sin\theta \\ -\frac{2}{d_0}\eta_2\cos\theta & -\frac{1}{d_0}\eta_1\cos\theta \end{bmatrix}\begin{bmatrix} \epsilon_1 \\ \epsilon_2 \end{bmatrix}.$$

The way each integrator chain is affected by the disturbances is depicted in Fig. 3, with $f_1^i(\theta,\eta_1)$ and $f_2^i(\theta,\eta,\epsilon_1,\epsilon_2)$ following from the above expressions for $\ddot{z}_i$ and $\dddot{z}_i$ $(i=1,2)$.

From standard linear system analysis and Fig. 3, it follows that, even for constant disturbances f_1^i and f_2^i, the steady-state error of the controlled output will be different from zero.

4.2 A modified linear controller for disturbance rejection

Consider a desired trajectory made of a straight line path with a kth order (canonical) polynomial timing law, i.e.,

$$z_{d1}(t) = \sum_{h=0}^{k} c_h \frac{t^h}{h!}, \quad z_{d2}(t) = c_0 + \rho z_{d1}(t),$$

where ρ is a proportionality factor.

Suppose that the closed-loop control system is of type k, i.e., is asymptotically stable and has zero steady-state error for a $(k-1)$th order canonical input (see, e.g., [10]). As a result, when $t \to \infty$, the vehicle orientation θ will converge to a constant value $\bar{\theta}$, its steady-state longitudinal velocity η_1 will be a $(k-1)$th polynomial function of time, while η_2 will go to zero. Therefore, disturbances f_1^i will become constant whereas disturbances f_2^i will be at most $(k-1)$th polynomial functions of time. In order to reject those disturbances at steady state, the linear stabilizer $C(s)$ in eq. (20) (equivalently, eq. (19)) should be modified so as to include k cascaded integrators.

If we focus on trajectories built up with 3rd order splines, we can design a controller that accomplish the goal of robust trajectory tracking by using three integrators. Taking advantage of a state feedback from vehicle position and velocity (which is equivalent to the presence of one realizable zero), and selecting two pairs of complex zeros, a real zero, and two real poles the resulting closed-loop system can be stabilized. Summarizing, the transfer function of the robust stabilizing

controller will have, for each input-output channel, the structure

$$C'(s) = (k_v s + k_p)\,\frac{(s+\alpha)\prod_{i=1}^{2}(s^2 + 2\omega_{ni}\zeta_i s + \omega_{ni}^2)}{s^3(s+p_1)(s+p_2)}. \tag{22}$$

Note that the above analysis holds only in the case of a straight line path, while for other kind of paths the disturbance equations are quite difficult to analyze. Nevertheless, the performance of the linear stabilizer (22) is satisfactory also for more general trajectories as illustrated in the following section.

5 Simulation Results

Numerical simulations of the tracking controller made of eqs. (12), (18), and (22) were performed with SIMULINK^{TM}, using the mechanical data characterizing the ATRV-2 robot. The vehicle dimensions are $a = 0.37$ m, $b = 0.55$ m, $2t = 0.63$ m, while the wheel radius is $r = 0.2$ m. The vehicle mass is $m = 116$ kg and its inertia is $I = 20$ kgm^2. The maximum achievable velocity is 2 m/s, while torque saturation for each motor occurs at 125 Nm, so that the maximum allowed torques τ_1 and τ_2 for each side of the vehicle are 250 Nm.

The desired trajectory is $z_{d1} = t$, $z_{d2} = -0.002t^3 + 0.1t^2 + 0.1t$ for $t \in [0, 50]$ sec, assigned to a point with $d_0 = 0.18$ m in eq. (14). The vehicle starts from the origin of frame F with a heading $\theta(0) = 10°$, i.e., it is initially out of the desired trajectory. Initial longitudinal and lateral (skidding) velocities are $\dot{x}(0) = \dot{y}(0) = 0.5$ m/s, with angular velocity $\dot{\theta}(0) = -2.2$ rad/s.

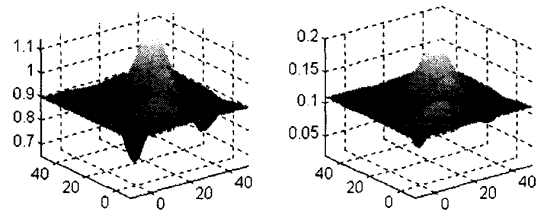

Figure 4: Fields of soil parameters μ and f_r

In order to validate the robustness of the tracking controller, we have simulated a virtual square (planar) terrain of side 50 m, with varying values of the friction coefficient μ and of the rolling resistance coefficient f_r, as shown in Fig. 4. The nonlinear controller uses instead constant estimates of soil parameters $\hat{\mu} = 0.895$ and $\hat{f}_r = 0.1$. The real values of μ and f_r encountered by the vehicle during its motion are plotted in Fig. 5.

The parameters of the robust linear stabilizer (22) are $p_1 = 9$, $p_2 = 5$, $\alpha = 1.5$, $\omega_{n1} = 1.5$, $\zeta_1 = 0.8$,

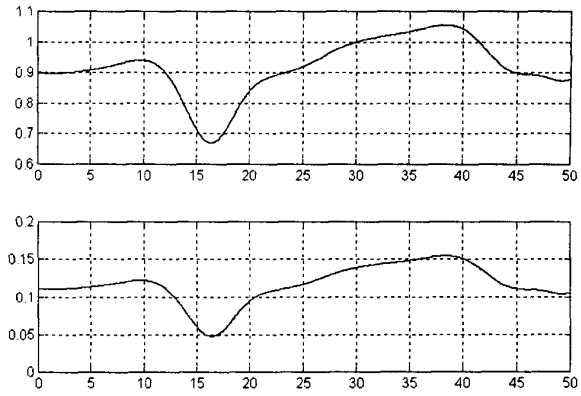

Figure 5: Actual values of μ and f_r during motion

$\omega_{n2} = 1$, $\zeta_2 = 1$, $k_v = 65$, and $k_p = 1.5k_v$, while $\xi(0) = 0$ in eq. (18).

Position and velocity errors are shown in Fig. 6, while the acceleration error and control torque behavior are presented in Fig. 7. Figure 8 shows a stroboscopic view of the vehicle tracking the desired trajectory on the virtual terrain. Gray levels indicate different values of soil parameters.

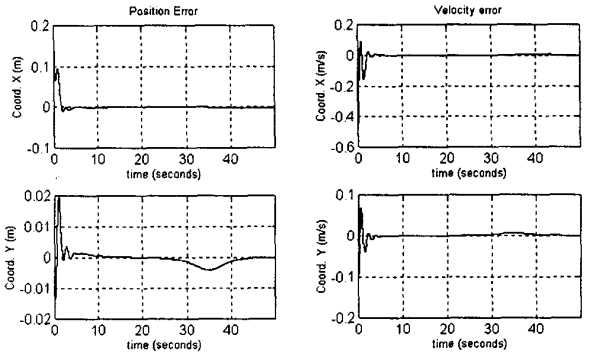

Figure 6: Position and velocity errors

The controller is able to recover from the initial error and stabilizes the vehicle to the desired trajectory, even if soil parameters are variable during motion. While position and velocity errors are rapidly compensated and remain very small, changes in soil parameters are more visible in the acceleration error, as expected. Note finally that the torques behavior is rather smooth, with initial peak values well within their feasible limits.

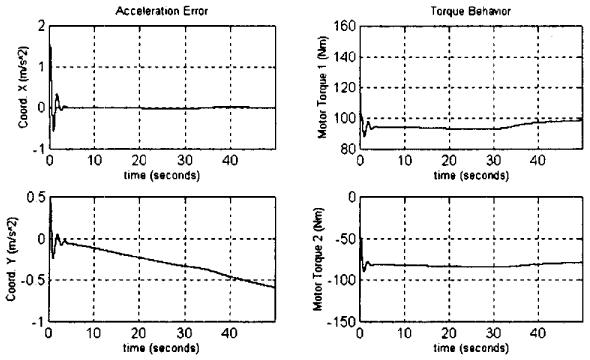

Figure 7: Acceleration error and torque behavior

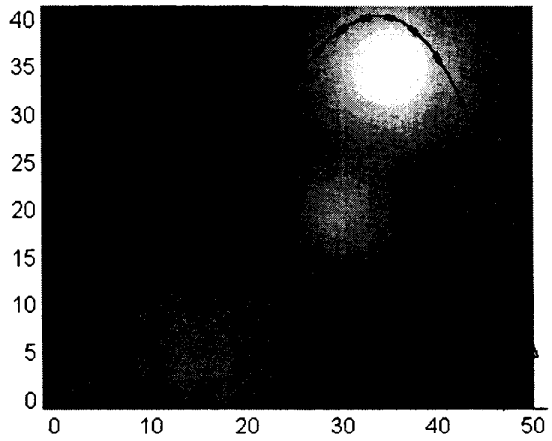

Figure 8: Stroboscopic view of robot motion

6 Conclusions

A robust controller for trajectory tracking of 4-wheel differentially driven vehicles has been presented. The control design minimizes unwanted lateral skidding, by imposing the longitudinal position of the instantaneous center of vehicle rotation. The controller is able to handle uncertain soil parameters.

The reported work constitutes one module of a more complex planning and control architecture that is going to be implemented for an ATRV-2 mobile robot. Among the extensions that should be included, we mention the control of 3D motion on uneven terrains and the use of global positioning sensors for measuring the actual robot state. For the latter problem, we have already simulated the presence of noise and/or transmission delays on state measurements, as would happen when using a GPS or a gyroscope for this purpose. Tracking performance remains satisfactory up to 60 ms delay and 10 cm peak position noise.

Acknowledgements

This work is supported by *Italian Space Agency*, under contract *ASI ARS-98-135*.

References

[1] Y. Fuke and E. Krotkov, "Dead reckoning for a lunar rover on uneven terrain," *1996 IEEE Int. Conf. on Robotics and Automation*, Minneapolis, MN, pp. 411–416, 1996.

[2] Z. Shiller, W. Serate, and M. Hua, "Trajectory planning of tracked vehicles," *1993 IEEE Int. Conf. on Robotics and Automation*, Atlanta, GA, pp. 796–801, 1993.

[3] A.T. Le, D.C. Rye, and H.F. Durrant-Whyte, "Estimation of track-soil interactions for autonomous tracked vehicles," *1997 IEEE Int. Conf. on Robotics and Automation*, Albuquerque, NM, pp. 1388–1393, 1997.

[4] A. De Luca, G. Oriolo, and C. Samson, "Feedback control of a nonholonomic car-like robot," in J.-P. Laumond (Ed.) *Robot Motion Planning and Control*, Lecture Notes in Control and Information Sciences, vol. 229, pp. 171–253, Springer-Verlag, London, 1998.

[5] B. d'Andrea-Novel, G. Campion, and G. Bastin, "Control of nonholonomic wheeled mobile robots by state feedback linearization," *Int. J. of Robotics Research*, vol. 14, no. 6, pp. 543–559, 1995.

[6] A.B. Will and S.H. Zak, "Modelling and control of an automated vehicle," *Vehicle System Dynamics*, vol. 27, pp. 131-155, 1997.

[7] J.Y. Wong, *Theory of Ground Vehicles*, John Wiley, New York, 1978.

[8] G. Campion, G. Bastin, and B. d'Andrea-Novel, "Structural properties and classification of kinematic and dynamic models of wheeled mobile robots," *IEEE Trans. on Robotics and Automation*, vol. 12, no. 1, pp. 47–62, 1996.

[9] A. Isidori, *Nonlinear Control Systems*, 3rd Edition, Springer-Verlag, London, 1995.

[10] J.J. D'Azzo and C.H. Houpis, *Linear Control System Analysis and Design*, 3rd Edition, McGraw-Hill, New York, 1988.